TOWARDS QUIKSCAT-DERIVED COASTAL WINDS

G. Grieco[1], *M. Portabella*[1], *A. Stoffelen*[2], *J. Vogelzang*[2], *A. Verhoef*[2]

[1]Barcelona Expert Centre (BEC), Institute of Marine Sciences (ICM-CSIC), Paseig Maritim de la Barceloneta 37, Barcelona (Spain)
[2]Royal Netherlands Meteorological Institute (KNMI), R&D Satellite Observations, 3731 GA De Bilt, The Netherlands

ABSTRACT

This paper presents the implementation of the Land Contribution Ratio (LCR) methodology for the pencil-beam scatterometer QuikSCAT, with the aim of improving the coastal sampling of the retrieved winds. This methodology is presented with two different models of the Spatial Response Function (SRF): the analytical model and the parameterized one, which is based on a pre-computed Look-up-Table (LUT) of SRFs provided by the Brigham Young University (BYU). Furthermore, a method to characterize the slice σ_0 noise (K_p) is presented and compared to the noise information provided in the full resolution QuikSCAT files. The preliminary results show that despite the overall consistency between the two SRF models, their discrepancies may induce LCR differences up to few percent. Furthermore, the K_p estimated by means of the slice Normalized Radar Cross Section (σ_0) is different from the K_p provided in the files, while such differencies are larger for certain slices and wind conditions. Such discrepancies can impact the wind field retrievals and, as such, should be further investigated.

***Index Terms*—** Coastal winds, pencil-beam scatterometers, QuikSCAT, Land Contribution Ratio

1. INTRODUCTION

Marine activities, sea state and port safety are affected by coastal winds. They also determine the local micro-climate, affecting advection and pollutants dispersion both in the atmosphere and in the ocean. Therefore, accurate coastal winds knowledge is crucial for both civil and scientific applications. In the last decade, many efforts have been devoted to enhance the coastal sampling of scatterometer-derived winds. The authors of [1] introduced the so called Land Contribution Ratio (LCR) methodology. They show how to optimally select the QuikSCAT coastal acquisitions that are not contaminated by land for the retrieval of the ocean surface wind field, and demonstrate how to improve the coastal sampling. The same approach has been used also for ASCAT acquisitions [2]. The authors of [2] also show how to speed-up the process by parameterizing the Spatial Response Function (SRF). High-resolution ASCAT derived winds have been validated in [3]. A more sophisticated LCR-based approach is proposed in [4] for ASCAT acquisitions, in which, a LCR-based Normalized Radar Cross Section (σ_0) correction scheme is applied to slightly contaminated ASCAT acquisitions, while the remaining are discarded. The Ocean and Sea Ice Satellite Application Facilities (OSI-SAF) of the European Organization for the Exploitation of the Meteorological Satellites (EUMETSAT) aims at releasing a QuikSCAT coastal product for the entire lifetime of the mission. This paper presents the preliminary steps towards this goal. In particular, this paper reports on the estimation of the SRF and the computation of the derived LCR, as described in [1]. Furthermore, a method to characterize the slice σ_0 noise (K_p) is proposed and the results are compared to the K_p information provided in the QuikSCAT level 1b (L1B) files.

Section 2 describes the methodology used for estimating the SRF and for characterizing the slice σ_0 noise. Section 3 describes the dataset used and section 4 shows the results. Finally, the discussion and the recommendations for future work are reported in section 5.

2. METHODOLOGY

2.1. LCR computation

The LCR is defined as the ratio between the footprint area contaminated by land and the total footprint area, as follows:

$$LCR = \frac{\sum_{xy} L_{xy} S_{xy}}{\sum_{xy} S_{xy}} \tag{1}$$

where L_{xy} is the binary Land-Sea Mask and S_{xy} is the SRF. The actual analytical QuikSCAT SRF has not been disclosed by the Jet Propulsion Laboratory (JPL), but a parameterized version has been kindly provided to us by Prof. Dave Long of the Brigham Young University (BYU). The parameterized version of the SRF can be obtained by following a two step process: a) the user queries a pre-computed look-up table (LUT) of SRF and, b) the obtained SRF is centered around the slice centroid. The LUT is queried by providing the azimuth antenna angle, the orbit time and the beam identifier. The centering procedure is necessary because the SRF obtained during step a) may be far from the slice centroid in a fashion that has no physical sense (private communication by Prof. Long). The analytical SRF has been computed by following the indications in [5]. The antenna gain pattern is not publicly available, therefore a cos^4-like approximate pattern has been used. The LSM used in eq. 1 is derived from the Global Self-consistent Hierarchical High-resolution Geography (GSHHG) data base, and has a spatial resolution of approximately 100 m [6].

2.2. slice σ_0 noise characterization

In order to characterize the slice σ_0 noise, 5 different levels of σ_0 have been considered for both horizontally polarized (H-pol) and vertically polarized (V-pol) beams. These levels range from low to high wind regimes. A 1 dB wide bin has been considered for each of the slice σ_0 levels. All slice σ_0 occurrences in the bin have been considered for the estimation of K_p ($\hat{K_p}$). K_p is defined as the ratio between the standard deviation of the slice σ_0 and the expected value of σ_0. Its analytical formulation is a second order polynomial function of the inverse of the signal-to-noise ratio (SNR) [7]. K_p is provided in the QuikSCAT L1B files. These values are compared with the those obtained with the following formulation:

$$\hat{K_p} = \frac{\sigma_{\hat{\sigma}_0}}{\sigma_0^{egg}}. \quad (2)$$

where $\sigma_{\hat{\sigma}_0}$ is the standard deviation of the measured slice σ_0 ($\hat{\sigma_0}$). σ_0^{egg} is a weighted averaged value over the entire QuikSCAT "egg" and is considered here as the expected slice σ_0 value. An egg is the set of slices corresponding to the same antenna pulse. In the case of QuikSCAT, it contains eight slices.

Only ocean acquisitions have been considered. The analysis has been limited to acquisitions in the latitude range between -60^o and 60^o in order to avoid any ice contaminations.

3. DATASET

Two QuikSCAT L1B full resolution files acquired on the 10^{th} of April 2007, whose orbit numbers are 40651 and 40653, have been used. Orbit 40653 is used for the validation of the LCR computation, while orbit number 40651 is used for the slice σ_0 noise characterization. Such kind of files are freely downloadable from the PODAAC web site [8]. The L1B files provide, among other, information about the slice and egg measurements (σ_0 and centroid position on the Earth surface), the satellite position and velocity, K_p, a set of Quality Control (QC) flags, the orbit time of the acquisition, the antenna azimuth angle and the beam identifier. Slice and egg positions together with the satellite position and velocity are necessary for the analytical computation of the SRF, while the slice centroid position, the antenna azimuth angle, the orbit time and the beam identifier are necessary for the computation of the LUT-derived SRF. QCed slice and egg information are also used for the slice σ_0 characterization, together with K_p for comparison. For what concerns QC, only some general quality flags are applied. Such flags relate to a) the reliability of the telemetry, b) the communication with the spacecraft, c) the quality of the scatterometer pulse, d) the convergence of the σ_0 cell (slice or egg) location algorithm, e) whether the temperature of the spacecraft is within the calibration coefficient range, f) wheter the frequency shift is within the range of the X factor table, g) whether an applicable attitude record was found, h) whether the interpolate ephemeris data are acceptable. The L1B files provide some additional quality flags regarding the slices. These flags consist of i) the slice σ_0 being negative, ii) the SNR being higher than a desired threshold value (SNR^{th}), iii) the peak antenna gain being higher than a desired threshold value and iv) the the slice centroid location being reliable. Those slices with the mentioned flags on are not used in the slice σ_0 noise characterization. In order to have an idea of their impact on the total number of acquisitions, inner (outer) beam acquisitions affected by the general quality flags amount to 0.6% (0.72%). If the slice quality flags are also applied, this percentage of filtered out data is 12.7% (3.45%). The reader may refer to [9] for further information.

4. RESULTS

Figure 1 shows the analytical (LUT-derived) 3dB SRF contours of each of the eight slices in black (red) in a coastal area of the Gulf of Taranto, south of Italy, and their centroids (black circles). The corresponding LCR values are reported to the side in black (red).

Figure 1 shows that the analytical and the LUT-derived contours are consistent with each other and that the LCR values are consistent with the coastline (in red). However, some differences are apparent. First, the LUT-derived contours are more irregular than the analytical ones, having a "saw teeth" feature which has no physical explanation. In addition, analytical contours may sometimes appear asymmetric with respect to the slice centroids. This feature is rather visible in the top most slice of figure 1. This is due to the fact that the iso-gain lines are not always symmetric with respect to the iso-range lines (not shown). Therefore, we claim this feature has a physical base. These minor differences may induce some significant differences in the LCR values up to a few percent, as shown in the figure. As such, they may significantly impact the LCR-based slice σ_0 correction scheme, and, in turn, the wind retrievals. This aspect deserves further investigation.

Figure 2 shows the scatter plot of the slice σ_0 versus the LCR for a set of QCed slices in a radius of 15 km from a wind vector cell grid in the Gulf of Taranto.

The set is separated according to the four "views" of

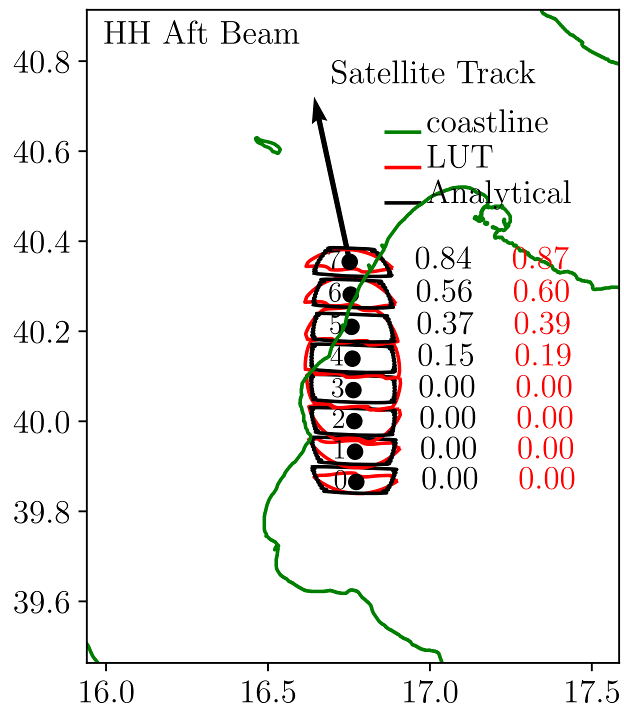

Fig. 1. Black (red) contours: QuikSCAT inner aft beam 3dB analytical (LUT-derived) SRF contours in the coastal area of the Gulf of Taranto, south of Italy. The slice index (0-based) is reported within each of the contours. Slice centroids are depicted with black circular markers. Black (red) text indicates the LCR values for each of the analytical (LUT-derived) contours. The black arrow depicts the flying direction of the spacecraft, while the coastline is depicted in green.

QuikSCAT: inner fore (HHF), inner aft (HHA), outer fore (VVF) and outer aft (VVA). In this figure, it is clear that: a) the higher the LCR is, the higher the slice σ_0 is, in an approximately linear fashion; and b) slice σ_0s are rather noisy. Indeed, for LCR equal to 0 (absence of any land contamination), the range of slice σ_0 values is around 30 dB, which seems excessive.
The analysis of the slice σ_0 noise shows that the higher the slice σ_0 level is, the lower $\hat{K}_p$ is (such as K_p), as expected. Indeed, the higher the slice σ_0 is, the higher the SNR is. In addition, the inner acquisitions are noisier than the outer ones. However, $\hat{K}_p$ and K_p may remarkably differ. The crosses (circles) in figure 3 show the trend of $\hat{K}_p$ (K_p) as a function of the slice index (from 0 to 7 in 0-based numbering), for each of the QuikSCAT views and for a slice σ_0 level approximately corresponding to a wind speed regime of 15 ms^{-1}.

It is clear that $\hat{K}_p$ has a parabolic trend with respect to the slice index. This feature is expected because peripheral slices are expected to be noisier than the central ones. K_p has a

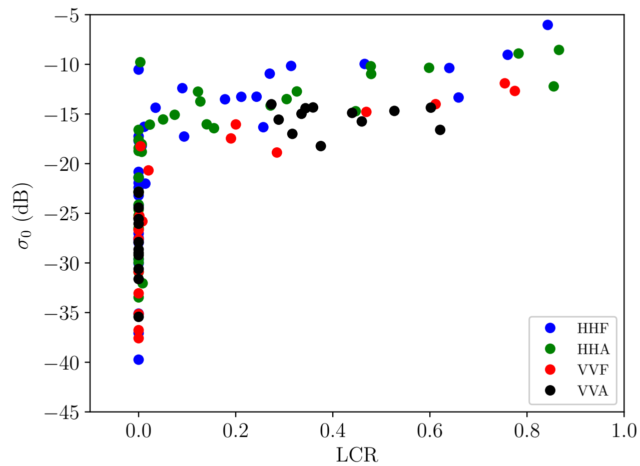

Fig. 2. Scatter plot of the slice σ_0 values versus the corresponding LCR values for a set of slices in the radius of 15 km from a coastal wind vector grid cell in the Gulf of Taranto, south of Italy. Marker colours represent the different ”views” of QuikSCAT. In the legend, HH (VV) stand for horizonally (vertically) polarized pulse and A (F) stands for aft (fore) beam.

rather different trend, being almost constant for slice indices higher than 2. Furthermore, for H-pol acquisitions, the K_p value is overestimated with respect to $\hat{K}_p$ for slice indices 0 and 1, and underestimated for slice indices 6 and 7. In addition, K_p is very noisy for low σ_0 levels (not shown). Finally, there are some inter-calibration issues between different slice indices (not shown). These issues are more severe for inner beam acquisitions.

5. CONCLUSIONS AND FUTURE WORK

This paper presents the first steps of the EUMETSAT OSI-SAF towards the development of a QuikSCAT-derived coastal wind product. In particular, this study reports on the implementation of the analytical and the LUT-derived SRFs for the computation of the LCR. Furthermore, it presents an analysis of the slice σ_0 noise. The preliminary results show that both SRF models have been successfully implemented and that the derived LCR is consistent with the coastline. However, some remarkable differences between both SRF models exist. These differences may lead to LCR variations of few percent. Considering that in [2], the authors filter out all the slices with LCR higher than 2%, it is expected that these differences may impact on the wind retrievals. This aspect deserves more investigation.
Furthermore, the slice σ_0s are shown to be very noisy, especially for the H-pol beam. The analysis of the slice σ_0 noise shows that $\hat{K}_p$ and K_p may remarkably differ. In particular, the K_p trend is not parabolic with respect to the central slice

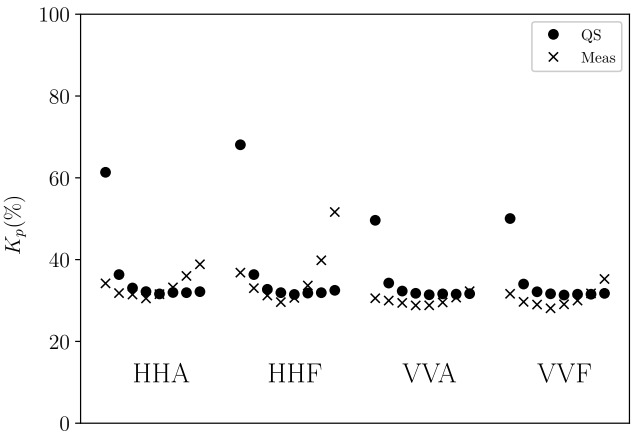

Fig. 3. Crosses (circles): average estimated K_p (provided in the L1B files) in percent as a function of the slice index, for a set of open ocean slice σ_0s approximately corresponding to a medium-high wind speed regime of 15 ms^{-1}. K_p values are separated according to the four QuikSCAT views.

indices, while $\hat{K}_p$ is. Furthermore, for H-pol acquisitions, K_p seems overestimated for slice indices 0 and 1, and underestimated for slice indices 6 and 7. In addition, the QuikSCAT slices seem to suffer from inter-calibration issues, which are more severe for the H-pol beam. The higher the distance is between the slices, the higher the bias is, which may reach 0.8 dB for H-pol acquisitions. In order to reduce such biases, an inter-calibration procedure is planned in the near future. Then, a K_p-weighed wind inversion scheme will be developed. Finally, an operational processor will be set-up and a climatological coastal wind dataset spanning the entire life cycle of QuikSCAT will be created.

Acknowledgements

This work was supported by the EUMETSAT Ocean & Sea Ice Satellite Application Facilities (OSI-SAF) Visiting Scientist projects VSA20_01 and VSA21_03 and by the Spanish R&D Plan through the Project L-BAND (reference ESP2017-89463-C3-1-R). The authors of this report would like to acknowledge Prof. Dave Long from the Brigham Young University for providing the Look-Up Table of pre-computed QuikSCAT Spatial Response Functions and for the precious support during the entire course of the project. Furthermore we would also like to acknowledge Dr. Bryan Stiles and Dr. Roy Scott Dumbar from the NASA Jet Propulsion Laboratory for providing guidance on the information content of the QuikSCAT L1B files.

6. REFERENCES

[1] M. P. Owen and D. G. Long, “Land-contamination compensation for quikscat near-coastal wind retrieval,” *IEEE Transactions on Geoscience and Remote Sensing*, vol. 47, no. 3, pp. 839–850, 2009.

[2] R. D. Lindsley, C. Anderson, J. Figa-Saldaña, and D. G. Long, “A parameterized ascat measurement spatial response function,” *IEEE Transactions on Geoscience and Remote Sensing*, vol. 54, no. 8, pp. 4570–4579, 2016.

[3] R. D. Lindsley, J. R. Blodgett, and D. G. Long, “Analysis and validation of high-resolution wind from ascat,” *IEEE Transactions on Geoscience and Remote Sensing*, vol. 54, no. 10, pp. 5699–5711, 2016.

[4] J. Vogelzang and A. Stoffelen, “Ascat land correction, report for the eumetsat ocean and sea ice saf,” Tech. Rep., Koninklijk Nederlands Meteorologisch Instituut, 2020, SAF/OSI/CDOP3/KNMI/TEC/TN/384.

[5] M. W. Spencer, C. Wu, and D. G. Long, “Improved resolution backscatter measurements with the seawinds pencil-beam scatterometer,” *IEEE Transactions on Geoscience and Remote Sensing*, vol. 38, no. 1, pp. 89–104, 2000.

[6] Pål Wessel and Walter H. F. Smith, “A global, self-consistent, hierarchical, high-resolution shoreline database,” *Journal of Geophysical Research: Solid Earth*, vol. 101, no. B4, pp. 8741–8743, 1996.

[7] R. E. Fischer, “Standard deviation of scatterometer measurements from space,” *IEEE Transactions on Geoscience Electronics*, vol. 10, no. 2, pp. 106–113, 1972.

[8] “https://podaac-opendap.jpl.nasa.gov/opendap/,” .

[9] Thorlabs, *QuikSCAT Science Data Product. User's Manual*, JPL NASA.